ELSEVIER

Journal of Alloys and Compounds 388 (2005) 208–214

Journal of ALLOYS AND COMPOUNDS

www.elsevier.com/locate/jallcom

Atomistic investigation on site preference and lattice vibrations of $Sm(Co,M)_{12}$ (M = Cr, Ti, V, Nb, Fe)

Jiang Shen[a,*], Ping Qian[a], Nan-Xian Chen[a,b]

[a] *Institute of Applied Physics, University of Science and Technology Beijing, Beijing 100083, China*
[b] *Department of Physics, Tsinghua University, Beijing 100084, China*

Received 2 June 2004; received in revised form 29 July 2004; accepted 29 July 2004

Abstract

The phase stability and site preference of the intermetallics $Sm(Co,M)_{12}$ (M = Cr, Ti, V, Nb, Fe) are evaluated by using interatomic pair potentials based on Chen's lattice inversion method. The calculated results show that substituting either Cr, Ti, V, Nb or Fe atoms makes the crystal cohesive energy of $Sm(Co,M)_{12}$ decrease markedly, proving that these atoms can stabilize $Sm(Co,M)_{12}$ with $ThMn_{12}$ structure. The calculated lattice constants coincide quite well with the experimental data. The order of site preference of these ternary elements T is 8*i*, 8*j* and 8*f* with the occupation of 8*i* corresponding to the greatest energy decreases. The properties related to lattice vibration, such as the phonon densities of states, specific heat and vibrational entropy, are also evaluated.

PACS: 71.20.Eh; 34.20.Cf; 63.20.Dj

Keywords: Interatomic potentials; Site preference; Lattice dynamics

1. Introduction

The intermetallic compounds of the $ThMn_{12}$-type have attracted much attention in the past due to their higher Curie temperatures and high magnetic moments [1–3]. As in the $R_2Fe_{14}B$ compounds, the substitution of Co for Fe in the $RFe_{10}M_2$ (R: rare-earth elements, M: other element) compounds leads to an enhancement in the Curie temperature [4]. In order to improve the magnetic properties of these compounds, the effects of substitution of Co for Fe in $R(Fe,Co)_{11}Ti$ and $R(Fe,Co)_{10}V_2$ have been investigated by several researchers [5–8]. Since the Co-based compounds can have high Curie temperature and large saturation magnetization, a complete substitution of Co for Fe in the $R(Fe,M)_{12}$ compounds to form the $R(Co,M)_{12}$ compounds with a structure identical to $R(Fe,M)_{12}$ has been carried out [9–11]. Recently, Chen et al. have performed serial theoretical studies on the phase stability, site preference and lattice parameters for the Fe-based rare-earth intermetallics $Gd(Fe,M)_{12}$ [12], $Sm(Fe,M)_{12}$ [13], $Nd(Fe,M)_{12}$ and $Nd(Fe,M)_{12}N_x$ [14], suggesting the validity of inverted pair potentials on the structure simulation of rare-earth compounds. In the present work, atomistic studies on the structural properties of Co-based rare-earth compounds $Sm(Co,M)_{12}$ are performed using inverted interatomic pair potentials. Emphasizing the statistical analysis of the phonon density of states (DOS), the Debye temperature of $Sm(Co,M)_{12}$ is evaluated based on the pair potentials.

2. Methodology

In principle, any interatomic pair potential can be obtained by a strict lattice inversion of cohesive energy curves. Acting on the lattice inversion method developed by Chen et al. [15,17,18], Chen and Ren [16] and Chen and co-worker [19], we can avoid parameter adjustment when deriving the

* Corresponding author. Tel.: +86 10 62322872; fax: +86 10 62322872.
E-mail address: shenj@sas.ustb.edu.cn (J. Shen).

0925-8388/$ – see front matter © 2004 Elsevier B.V. All rights reserved.
doi:10.1016/j.jallcom.2004.07.045

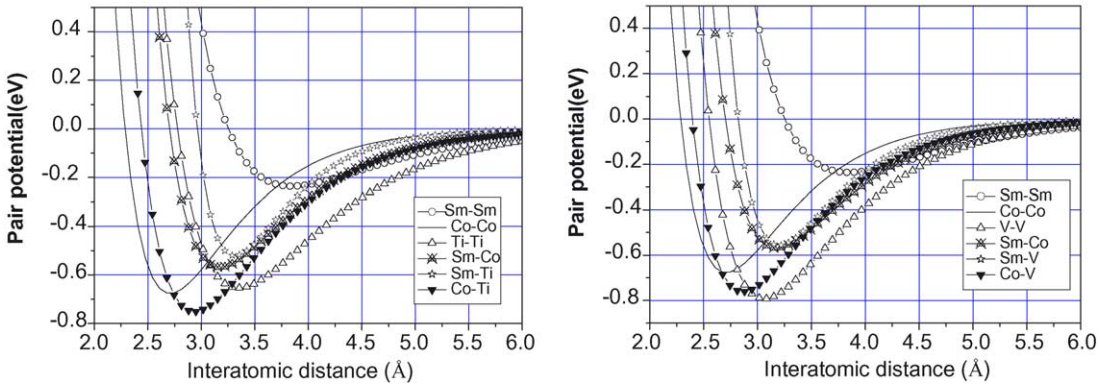

Fig. 1. Some pair potentials used in $Sm(Co,M)_{12}$.

interatomic potentials. The method can be summarized as follows: it assumes that the total cohesive energy per atom in a perfect crystal can be expressed as the sum of pair potentials, i.e.

$$E(x) = \frac{1}{2}\sum_{R_i \neq 0} \Phi(R_i) = \frac{1}{2}\sum_{n=1}^{\infty} r_0(n)\Phi[b_0(n)x] \quad (1)$$

where x is the nearest-neighbor interatomic distance, R_i is the lattice vector of the ith atom, $r_0(n)$ is the nth neighbor coordination number, and $b_0(n)x$ is the nth neighbor distance. We extend the series, $\{b_0(n)x\}$, into a multiplicative semigroup, then the general equation for pair potential $\Phi(x)$ can be expressed as

$$E(x) = \frac{1}{2}\sum_{n=1}^{\infty} r(n)\Phi[b(n)x] \quad (2)$$

where

$$r(n) = \begin{cases} r(b_0^{-1}[b(n)]), & b(n) \in \{b_0(n)\} \\ 0, & b(n) \notin \{b_0(n)\} \end{cases} \quad (3)$$

and the pair potential from the inversion can be expressed as

$$\Phi(x) = 2\sum_{n=1}^{\infty} I(n)E[b(n)x] \quad (4)$$

where $I(n)$ is determined by

$$\sum_{b(n)|b(k)} I(n) r\left[b^{-1}\left[\frac{b(k)}{b(n)}\right]\right] = \delta_{k_1} \quad (5)$$

$I(n)$ is uniquely determined by crystal structure geometry, not related to the concrete element category. Thus, the interatomic pair potentials can be obtained from the known cohesive energy function $E(x)$ [12–14]. Several important relevant interatomic pair potential curves are shown in Fig. 1, which are fitted by Morse function, that is

$$\Phi(x) = D_0(e^{-\gamma(x/R_0-1)} - 2e^{-(\gamma/2)(x/R_0-1)}) \quad (6)$$

where D_0 is the depth of potential, R_0, γ are parameters.

3. Phase stability and site preference

Based on the atomic sites and lattice parameters of any existing experimental structure close to $ThMn_{12}$-type with the *I*4/*mmm* space group, the initial structures are constructed with Accelrys Cerius2 modeling software. Then, energy minimization is carried out using the conjugate-gradient method on the basis of calculated interatomic potentials with the cut-off radius of potentials of 14 Å. Despite the fact that the virtual binary structure of $SmCo_{12}$ is metastable, it can be considered as the intrinsic structure of $Sm(Co,M)_{12}$. In the calculation, the initial lattice parameters of $SmCo_{12}$ are set arbitrarily (Table 1), and then the deformed system is relaxed

Table 1
Determination of lattice parameters of $SmCo_{12}$

Initial state		Final state	
a, *b*, *c* (Å)	*α*, *β*, *γ* (°)	*a*, *b*, *c* (Å)	*α*, *β*, *γ* (°)
24, 20, 12	90, 60, 90	8.393, 8.393, 4.746	90, 90, 90
3.6, 3.9, 3.6	130, 90, 90	8.393, 8.393, 4.746	90, 90, 90
10, 11, 12	90, 70, 65	8.393, 8.393, 4.746	90, 90, 90
8.393, 8.393, 8	60, 70, 100	8.393, 8.393, 4.746	90, 90, 90
8.393, 8.393, 4.768	140, 65, 90	8.393, 8.393, 4.746	90, 90, 90
18, 18, 15	90, 90, 90	8.393, 8.393, 4.746	90, 90, 90
16, 19, 7.5	50, 70, 50	8.393, 8.393, 4.746	90, 90, 90

using energy minimization method. The results suggest that the space group maintains *I*4/*mmm*, and the lattice constants after stabilization are a = 8.441 Å, c = 4.798 Å. The presence of a certain amount of randomness of the initial structure and the stability of the final structure illustrate $SmCo_{12}$ has a topological invariability with respect to the stable $Sm(Co,M)_{12}$. It also demonstrates that the inverted pair potentials are reliable for the study of the structural materials properties.

In the ternary compounds $Sm(Co,M)_{12}$, the phase stability and site preference are judged by the energy in this part. If the substitution of ternary elements T for Co makes the cohesive energy of $Sm(Co,M)_{12}$ low enough, the ternary elements could stabilize the compound. Furthermore, T would preferentially occupy the site, so that the cohesive energy would decrease most strongly. In the course of the calculation, firstly, Co atoms in each site are replaced by T atoms of different concentrations. Then, energy minimization process is applied to relax the ternary system under the interaction of the potentials. Thus, the average energy of final structure can be investigated and compared. The calculated crystal energy is the average of 30 samples and is shown in Fig. 2. From Fig. 2, it can be seen that adding either Cr, Ti, V, Nb or Fe atoms makes the cohesive energy of $Sm(Co,M)_{12}$ decrease markedly, illustrating that each of these elements can stabilize the crystal structure and that the stabilized phases exist. The cohesive energy decreases most significantly when the ternary elements T preferentially occupy the 8*i* sites, less significantly if the T atoms occupy the 8*j* sites, and behaves abnormally when occupying the 8*f* sites. All of the above results correspond well to the experiment [20,21] and the T atoms have the same site preference in Co-based as in Fe-based compounds [12,13].

According to the results for site preference, the lattice constants for $Sm(Co,M)_{12}$ are calculated when the 8*i* sites are randomly occupied by T atoms. The calculated results are listed in Table 2, together with the experimental data [22,23]. From Table 2, one can see that our results for $Sm(Co,M)_{12}$ are in agreement with experiment. Furthermore, the structural stability of $Sm(Co,M)_{12}$ is tested by some methods including global deformation and random atom shift. In the processes, the global deformation includes stretching, compressing, shearing and a mixture of these ways. The random atom shift means that each atom in the model is shifted from its equilibrium position randomly. All distorted models will be relaxed under the control of pair potential using the energy minimization method. The calculated results are listed in Table 2. From the calculated results, it can be seen that the distorted system can restore the same final structure. In order to check the structural stability at high temperature, the high temperature disturbance is used with molecular dynamics. The constant-*NPT* molecular dynamics is applied using the method of Berendsen et al. [24] for 10,000 steps, with P = 1 atm, t = 0.001 ps, dynamic simulation for $SmCo_{10.14}Ti_{1.86}$ is carried out at temperatures of 300, 500 and 700 K. After

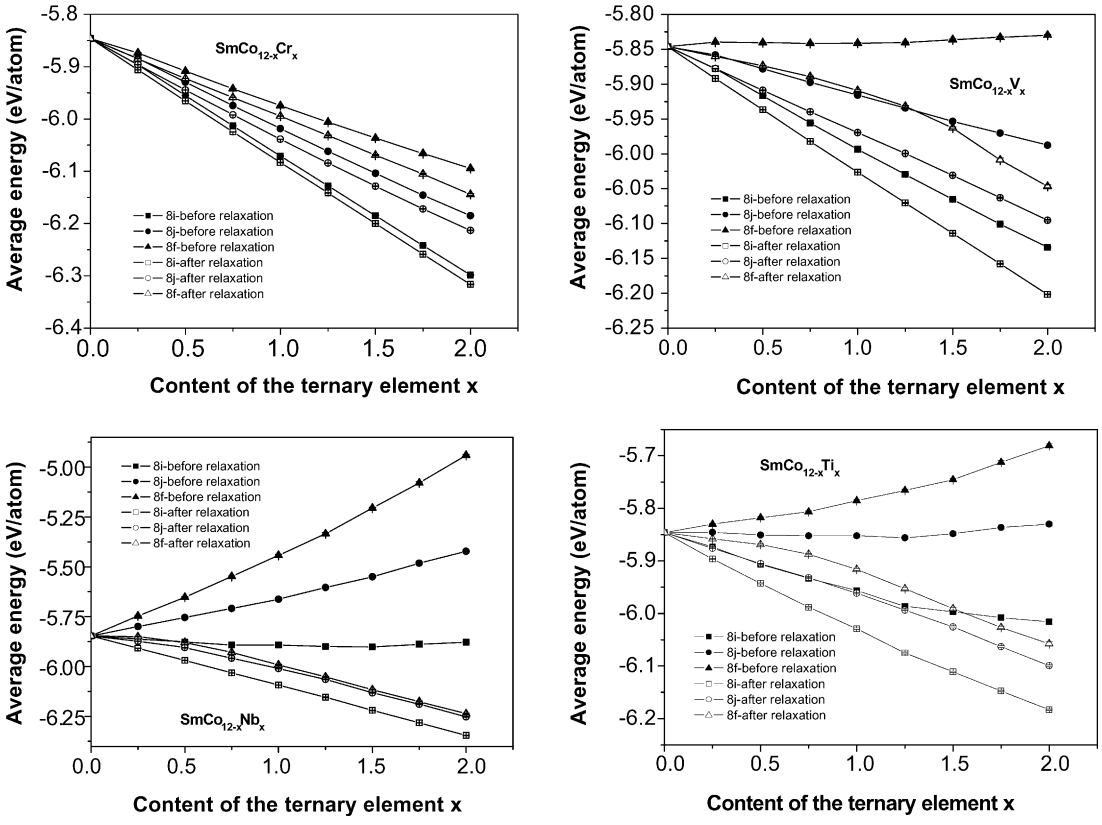

Fig. 2. Site preference of $Sm(Co,M)_{12}$.

Table 2
Comparison between the experimental [22,23] and calculated structure of $SmCo_{12-x}T_x$

Compounds	Space group	Calculated a (Å)	Experimental a (Å)	Calculated c (Å)	Experimental c (Å)
$SmCo_{11}Cr_1$	*I*4/*mmm*	8.405	–	4.761	–
$SmCo_{11}Nb_1$	*I*4/*mmm*	8.558		4.841	
$SmCo_{10}Fe_2$	*I*4/*mmm*	8.403		4.778	
$SmCo_{9.8}V_{2.2}$	*I*4/*mmm*	8.448	8.3802 (1)	4.784	4.7047 (1)
$SmCo_{10.51}Ti_{1.49}$	*I*4/*mmm*	8.539	8.426	4.810	4.741
$SmCo_{10.39}Ti_{1.61}$	*I*4/*mmm*	8.560	8.433	4.812	4.746
$SmCo_{10.26}Ti_{1.74}$	*I*4/*mmm*	8.563	8.438	4.820	4.748
$SmCo_{10.14}Ti_{1.86}$	*I*4/*mmm*	8.582	8.433	4.825	4.750
$SmCo_{10.05}Ti_{1.95}$	*I*4/*mmm*	8.594	8.447	4.8291	4.752
$SmCo_{9.8}V_{2.2}$ (0.6 Å)[a]	*I*4/*mmm*	8.448	–	4.784	–
$SmCo_{11}Cr_1$ (0.6 Å)[a]	*I*4/*mmm*	8.405	–	4.761	–
$SmCo_{10.14}Ti_{1.86}$ (0.6 Å)[a]	*I*4/*mmm*	8.582	8.433	4.825	4.750
$SmCo_{10.14}Ti_{1.86}$ (300 K)	*I*4/*mmm*	8.590		4.834	
$SmCo_{10.14}Ti_{1.86}$ (500 K)	*I*4/*mmm*	8.608		4.835	
$SmCo_{10.14}Ti_{1.86}$ (700 K)	*I*4/*mmm*	8.612		4.837	

[a] Relaxation results with atom random shift by 0.6 Å.

reaching equilibrium, the crystal symmetry can be identified as *I*4/*mmm* space group in a certain range, and the lattice constants change little with respect to the temperature (Table 2). Thus, the structural stability is again verified. These results further verify that the above calculations are self-consistent and reasonable. So, it can be inferred from the above calculations that the site preference and lattice constants of $Sm(Co,M)_{12}$ evaluated using the interatomic pair potentials agree well with experiment, which demonstrates that the potentials are reliable.

The behaviors of ternary elements substitution can be explained by the analysis and comparison of interatomic pair potentials in $Sm(Co,M)_{12}$. When a small amount of ternary elements T substitute the Co atoms in $SmCo_{12}$, the ternary elements are mostly surrounded by the Co atoms. The Sm atoms are not their own nearest neighbor atoms, and the occasions on which T atoms are their own nearest neighbors are truly rare. Therefore, the role of $\Phi_{Sm-Sm}(r)$ and $\Phi_{T-T}(r)$ is negligible when considering the nearest neighbor effect. It is the differences between $\Phi_{Co-T}(r)$ and $\Phi_{Co-Co}(r)$ that determine the energy difference caused by the substitution. We choose T = Ti as an example. As shown in Fig. 1, the potential values are important in the range of $2.3 < r < 4.4$ Å. Notice that $\Phi_{Co-Ti}(r)$ intersects with $\Phi_{Co-Co}(r)$ at about r = 2.7 Å. When the interatomic distance $r < 2.7$ Å, the system energy will increase with Ti substituting for Co due to $\Phi_{Co-Ti}(r) > \Phi_{Co-Co}(r)$, it is unfavorable for the substitution. In the range of $2.7 < r < 4.4$ Å, $\Phi_{Co-Ti}(r) < \Phi_{Co-Co}(r)$, it is favorable for energy decrease. The substitution behavior can be qualitatively explained by carrying out a cluster analysis of the surroundings. If we take the 8*i* site as the center of a cluster, the number of Co atoms inside a sphere of radius 2.7 Å is about 9. The number of Co atoms inside a range of $2.7 < r < 4.4$ Å is about 22. Thus, Ti occupying the 8*i* sites is most beneficial in terms of energy minimization. The site preference behavior at 8*i* and 8*j* sites can be easily explained by similar analysis.

4. Phonon density of states

Phonon density of states reflects the lattice vibration properties. From DOS, one can derive important thermodynamic parameters as specific heat, the Debye temperature. Starting with the inverted interatomic potentials and lattice dynamics theory, we calculate the total phonon densities of states, as well as the partial DOS projected to different elements in $Sm(Co,M)_{12}$.

The calculated DOS of $SmCo_{12}$ and $Sm(Co,M)_{12}$ are shown in Fig. 3(a–d). The DOS of Fig. 3 is calculated by using 936 k-points in 1/8 of the first Brillouin zone of simple tetragonal lattice. The cut-off distance of force constants is set at 6 Å. Fig. 3(a) shows that the highest frequency of $SmCo_{10}Cr_2$ is 10.92 THz and there are five apexes around 2.96, 3.69, 4.61, 5.62 and 7.38 THz, respectively. For two localized modes, the frequencies are higher than 8.31 THz. The high frequency vibrations and the high frequency localized modes are mainly contributed by the Co atoms. And the Sm atoms only contribute to the lower frequency modes. It can be seen from Fig. 3 that, when T atoms substitute for Co atoms at 8*i* sites in $Sm(Co,M)_{12}$, the contribution of the ternary element to frequency modes is the same as that of Co in manner, but with a smaller amplitude. Qualitative analysis can be conducted on the vibration modes from interaction potentials (Fig. 1) and the nearest neighbor distances between the atoms. As shown in Fig. 1, the very strong interaction between Co and Co at their nearest distance (2.32 Å) causes Co to vibrate at high frequencies. For Sm atoms, as the distance between Sm and its nearest Co is 3.39 Å, atoms cannot excite more modes with higher frequency due to the infirm interaction in this range and the heavy mass of Sm. When T substitutes for Co in 8*i* site, there is one nearest Co neighbor at the 8*i* site, and there are four second nearest Co neighbors at the 8*i* site, two at the 8*j* site and four at the 8*f* site in the $Sm(Co,M)_{12}$ compounds. The distances between the T atom at 8*i* and these atoms are 2.32 Å to the single 8*i* site, 2.80 Å

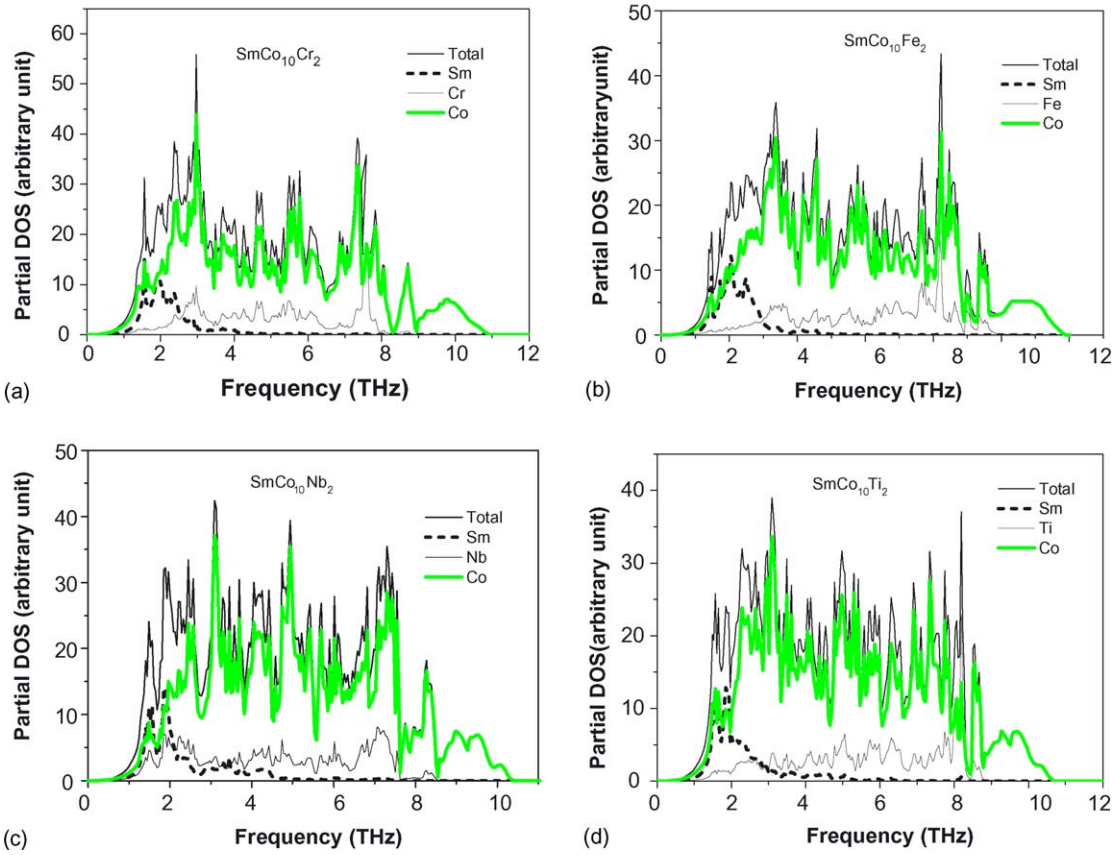

Fig. 3. Phonon densities of states of $Sm(Co,M)_{12}$.

to the other four 8*i* sites, 2.70 Å to the 8*j* sites and 2.60 Å to the four 8*f* sites. Consequently, the neighbor distances at the occupied 8*i* site are mainly between 2.60 and 2.80 Å. It can be inferred from Fig. 1 that at a distance of about 2.70 Å, the Co–Co interaction is nearly the Co–T interaction. Hence, the frequency modes of the ternary elements are almost the same with Co in shape, but the amplitude is much smaller because the content of ternary elements is small.

The calculation of specific heat $C_v(T)$ and the vibrational entropy $S(T)$ can be made by using the following formulae

$$C_v(T) = 3Nk_B \int_0^\infty \frac{(\hbar\omega/k_BT)^2 e^{\hbar\omega/k_BT}}{(e^{\hbar\omega/k_BT}-1)^2} g(\omega)\,d\omega$$

and

$$S(T) = \int_0^T \frac{C_v(T')}{T'}\,dT'$$

In the conventional Debye model, the Debye temperature Θ_D can be defined by $\hbar\omega_m = k_B\Theta_D$. The specific heat can be written as

$$C_v = 3Nk_B\left(\frac{T}{\Theta_D}\right)^3 \int_0^{\Theta_D/T} \frac{x^4 e^x}{(e^x-1)^2}\,dx$$

where $x = \hbar\omega_m/k_B\Theta_D$. The calculated specific heat, vibrational entropy and Debye temperature of $Sm(Co,M)_{12}$ are shown in Figs. 4–6, respectively. It can be seen in Figs. 4–6 that the variation of the specific heat, Debye temperature and entropy versus temperature indicate the vibrational properties are different for $Sm(Co,M)_{12}$ in the entire temperature range. Table 3 shows the Debye temperature near 0 K and at 300 K for $Sm(Co,M)_{12}$ (T = Cr, Ti, V, Nb, Fe). The Debye temperature reflects the property of the materials at the lower temperature and lower frequency. The Debye temperature of $SmCo_{12}$ is 394 K near 0 K. The Debye temperature

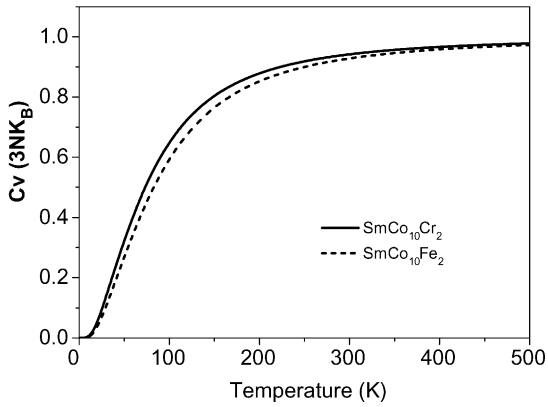

Fig. 4. Specific heat of $SmCo_{10}Cr_2$ and $SmCo_{10}Fe_2$.

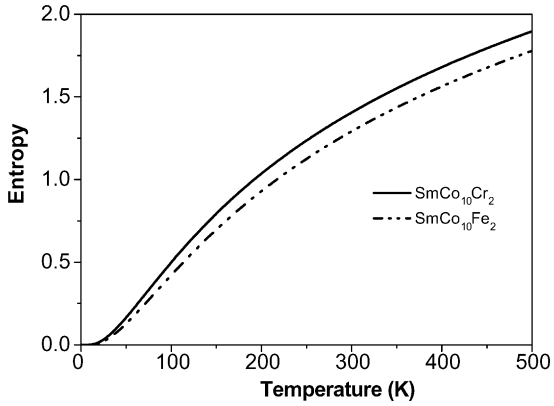

Fig. 5. Vibrational entropy of $SmCo_{10}Cr_2$ and $SmCo_{10}Fe_2$.

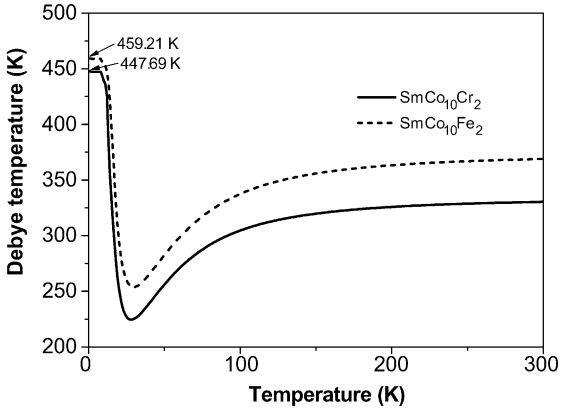

Fig. 6. Debye temperature of $SmCo_{10}Cr_2$ and $SmCo_{10}Fe_2$.

increases when Co atoms are substituted by the ternary elements T (T = Cr, Ti, V, Nb, Fe) in the $SmCo_{10}T_2$ compounds, and the increase is most noticeable when T = Fe. Hence, the ternary elements T (T = Cr, Ti, V, Nb, Fe) can partly influence the thermodynamic properties of these kinds of materials, and Fe may play an important role in the lower-temperature properties of these materials. Unfortunately, in the existing literature, there are not any observational data on the Debye temperature of the $Sm(Co,M)_{12}$ compounds. Therefore, the above calculation results have not yet been verified by experiments.

Table 3
Debye temperature Θ_D (K) of $SmCo_{12-x}T_x$ at near 0 K and at 300 K

Compounds	Θ_D (K)	
	Near 0 K	At 300 K
$SmCo_{10}Cr_2$	447.69	330.38
$SmCo_{10}Fe_2$	459.21	368.93
$SmCo_{10}Nb_2$	430.31	362.22
$SmCo_{10}Ti_2$	451.61	337.87
$SmCo_{10}V_2$	453.12	336.48

5. Conclusion

In this work, the distribution of ternary elements T in $Sm(Co,M)_{12}$ is evaluated by using the interatomic potentials. The calculated result demonstrates that the ternary elements T (T = V, Ti, Cr, Nb, Fe) substitute Co atoms in the 8*i* sites, the crystal cohesive energy of $Sm(Co,M)_{12}$ decreases most significantly. Therefore, the T atoms preferentially occupy the 8*i* sites. We have also utilized the same potential parameters to evaluate the phonon density of states of $Sm(Co,M)_{12}$, and obtained its specific heat, vibrational entropy and Debye temperature. In summary, the inverted potentials are effective to investigate the site preference, phase stability and to predict the properties of these materials with complex structures. As a last point, it should be mentioned that current work does not include many-body interaction and magnetic effect, and that might be the next objective of our work.

Acknowledgements

The authors would like to thank the stimulating discussions with Professor F.M. Yang, D.B. Zhang and Y.M. Kang. The present work is supported by National 973 Project TG2000067101 and TG2000067106.

References

[1] K. Ohashi, Y. Tawara, R. Osugi, J. Sakurai, Y. Komura, J. Less-Common Met. 139 (1988) L1.
[2] B.P. Hu, K.Y. Wang, Y.Z. Wang, Z.X. Wang, Q.W. Yan, P.L. Zhang, X.D. Sun, Phys. Rev. B 51 (1995) 2905.
[3] V.Yu. Bodriakov, T.I. Ivanova, S.A. Nilitin, I.S. Tereshina, J. Alloys Compd. 259 (1997) 265.
[4] K.H.J. Buschow, D.B. de Mooij, M. Brouha, H.H.A. Smith, R.C. Thiel, IEEE Trans. Magn. MAG-24 (1988) 1611.
[5] V.K. Sinha, S.F. Cheng, W.E. Wallace, S.G. Sankar, J. Magn. Magn. Mater. 81 (1989) 227.
[6] M. Jurczyk, O.D. Chistjakov, J. Magn. Magn. Mater. 82 (1989) 239.
[7] M. Jurczyk, G.K. Nicolaides, K.V. Rao, J. Magn. Magn. Mater. 94 (1991) L6.
[8] M. Jurczyk, G.K. Nicolaides, K.V. Rao, J. Appl. Phys. 70 (1991) 6110.
[9] X. Xie, S.A. Shaheen, J. Magn. Magn. Mater. 118 (1993) L6.
[10] J.H.V.J. Brabers, G.F. Zhou, F.R. de Boer, K.H.J. Buschow, J. Magn. Magn. Mater. 118 (1993) 339.
[11] K. Ohashi, H. Ido, K. Konno, Y. Yoneda, J. Appl. Phys. 70 (1991) 10.
[12] N.X. Chen, J. Shen, X.P. Su, J. Phys.: Condens. Matter 13 (2001) 2727.
[13] N.X. Chen, S.Q. Hao, Y. Wu, J. Shen, J. Magn. Magn. Mater. 233 (2001) 169.
[14] S.Q. Hao, N.X. Chen, Phys. Lett. A 297 (2002) 110.
[15] N.X. Chen, Z.D. Chen, Y.C. Wei, Phys. Rev. E 55 (1) (1997) R5.
[16] N.X. Chen, G.B. Ren, Phys. Rev. B 45 (1992) 8177.
[17] N.X. Chen, X.J. Ge, W.Q. Zhang, F.W. Zhu, Phys. Rev. B 57 (1998) 14203.
[18] W.Q. Zhang, Q. Xie, X.J. Ge, N.X. Chen, J. Appl. Phys. 82 (2) (1997) 578.
[19] X.J. Ge, N.X. Chen, J. Appl. Phys. 85 (7) (1999) 3488.

[20] K.H.J. Buschow, J. Appl. Phys. 63 (8) (1988) 3130.
[21] R.B. Helmholdt, J.J.M. Vleggaar, K.H.J. Buschow, J. Less-Common Met. 138 (1988) L11.
[22] W.Q. Wang, J.L. Wang, N. Tang, F.Q. Bao, G.H. Wu, F.M. Yang, H.M. Jin, Acta Phys. Sin. 50 (4) (2001) 756.
[23] W.F. Liu, G.H. Rao, H.F. Yang, Z.W. Ouyang, G.Y. Liu, X.M. Feng, J.K. Ling, J. Alloys Compd. 361 (2003) 62.
[24] H.J.C. Berendsen, J.M.P. Postma, W.F. van Gunstern, J. Chem. Phys. 81 (1984) 3684.